

Supplementary material for *Toroidal Moments in Confined Nanomagnets and their Impact on Magnonics*

F. Brevis,^{1,*} L. Körber,² B. Mimica-Figari,¹ R. A. Gallardo,¹ A. Kákay,³ and P. Landeros^{1,†}

¹*Departamento de Física, Universidad Técnica Federico Santa María, Avenida España 1680, Valparaíso, Chile*

²*Radboud University, Institute of Molecules and Materials,
Heyendaalseweg 135, 6525 AJ Nijmegen, The Netherlands*

³*Helmholtz-Zentrum Dresden-Rossendorf, Institute of Ion Beam Physics and Materials Research,
Bautzner Landstr. 400, 01328 Dresden, Germany*

(Dated: June 17, 2025)

This Supplementary Material provides a detailed account of the main calculations, starting with the derivation of the surface toroidal moment. Next, the expressions for the toroidal moment arising from well-known magnetic textures are computed.

I. ANALYTICAL DERIVATION OF THE SURFACE TOROIDAL MOMENT

The toroidal moment associated with any current proposed by Dubovik and Tugushev [1] is

$$\boldsymbol{\tau} = \frac{1}{10} \int dV [\mathbf{r}(\mathbf{r} \cdot \mathbf{J}) - 2r^2 \mathbf{J}]. \quad (1)$$

In order to investigate the connection between the magnetization (\mathbf{M}) and the toroidal moment ($\boldsymbol{\tau}$), consider that a magnetization distribution may create a bound current (\mathbf{J}_b), defined as

$$\mathbf{J}_b(\mathbf{r}) = \nabla \times \mathbf{M}, \quad (2)$$

and in the absence of free and polarization currents, $\mathbf{J} = \mathbf{J}_b$. Replacing this expression into the Eq (1),

$$\boldsymbol{\tau} = \frac{1}{10} \int dV [\mathbf{r}(\mathbf{r} \cdot (\nabla \times \mathbf{M})) - 2r^2(\nabla \times \mathbf{M})]. \quad (3)$$

As $\nabla \times \mathbf{r} = 0$, then, the divergence of a cross-product can be written as

$$\nabla \cdot (\mathbf{r} \times \mathbf{M}) = -\mathbf{r} \cdot (\nabla \times \mathbf{M}). \quad (4)$$

On the other hand, the curl of the product between a scalar function ψ and a vector function \mathbf{M} can be expanded as

$$\nabla \times (\psi \mathbf{M}) = \psi(\nabla \times \mathbf{M}) + (\nabla \psi) \times \mathbf{M}. \quad (5)$$

Considering that $\psi = -2r^2$, the second term in Eq. 3 gives

$$-2r^2(\nabla \times \mathbf{M}) = -2\nabla \times (r^2 \mathbf{M}) + 4\mathbf{r} \times \mathbf{M}, \quad (6)$$

then, the toroidal moment becomes

$$\boldsymbol{\tau} = \frac{1}{10} \int dV [-\mathbf{r}[\nabla \cdot (\mathbf{r} \times \mathbf{M})] - 2\nabla \times (r^2 \mathbf{M}) + 4\mathbf{r} \times \mathbf{M}]. \quad (7)$$

From vector calculus identities,

$$\int_V dV \psi \nabla \cdot \mathbf{A} = \oint_S \psi \mathbf{A} \cdot d\mathbf{S} - \int_V dV \mathbf{A} \cdot \nabla \psi. \quad (8)$$

* felipe.brevis@usm.cl

† pedro.landeros@usm.cl

On the other hand, in Cartesian coordinates, it can be considered that,

$$\int dV \mathbf{r} [\nabla \cdot (\mathbf{r} \times \mathbf{M})] = \hat{r}_i \int dV r_i [\nabla \cdot (\mathbf{r} \times \mathbf{M})] \quad (9)$$

Where $r_i = x, y, z$, and the Einstein notation is used. Considering $\psi = r_i$ and $\mathbf{A} = \mathbf{r} \times \mathbf{M}$, then

$$\int_V dV r_i \nabla \cdot (\mathbf{r} \times \mathbf{M}) = \oint_S r_i (\mathbf{r} \times \mathbf{M}) \cdot d\mathbf{S} - \int_V dV (\mathbf{r} \times \mathbf{M}) \cdot \nabla r_i, \quad (10)$$

but we have that $\nabla r_i = \hat{r}_i$, then

$$\int_V dV r_i \nabla \cdot (\mathbf{r} \times \mathbf{M}) = \oint_S r_i (\mathbf{r} \times \mathbf{M}) \cdot d\mathbf{S} - \int_V dV (\mathbf{r} \times \mathbf{M})_i, \quad (11)$$

and adding the three components,

$$\hat{r}_i \int_V dV r_i \nabla \cdot (\mathbf{r} \times \mathbf{M}) = \hat{r}_i \oint_S r_i (\mathbf{r} \times \mathbf{M}) \cdot d\mathbf{S} - \int_V dV (\mathbf{r} \times \mathbf{M}). \quad (12)$$

Replacing the obtained result into the toroidal moment in Eq. 7,

$$\boldsymbol{\tau} = -\frac{1}{10} \oint_S dS \mathbf{r} [(\mathbf{M} \times \mathbf{n}) \cdot \mathbf{r}] - \frac{2}{5} \int_V dV \nabla \times (r^2 \mathbf{M}) + \frac{1}{2} \int_V dV \mathbf{r} \times \mathbf{M}. \quad (13)$$

The volume integral of the curl of a function, which can be obtained from the Gauss Theorem, is

$$\int_V dV \nabla \times \mathcal{G} = - \oint_S \mathcal{G} \times d\mathbf{S}. \quad (14)$$

By considering that $\mathcal{G} = r^2 \mathbf{M}$ and $d\mathbf{S} = \mathbf{n} dS$ where \mathbf{n} is the unit vector normal to the surface,

$$\boldsymbol{\tau} = -\frac{1}{10} \oint_S dS \mathbf{r} [(\mathbf{M} \times \mathbf{n}) \cdot \mathbf{r}] + \frac{1}{5} \oint_S dS r^2 (\mathbf{M} \times \mathbf{n}) + \frac{1}{2} \int_V dV \mathbf{r} \times \mathbf{M}. \quad (15)$$

It follows that $\mathbf{M} \times \mathbf{n}$ corresponds to the bound surface current \mathbf{K}_b [2], and the toroidal moment is

$$\boldsymbol{\tau} = \frac{1}{2} \int_V dV (\mathbf{r} \times \mathbf{M}) - \frac{1}{10} \oint_S dS [\mathbf{r}(\mathbf{r} \cdot \mathbf{K}_b) - 2r^2 \mathbf{K}_b]. \quad (16)$$

Then, the toroidal moment splits into two contributions, $\boldsymbol{\tau} = \boldsymbol{\tau}^v + \boldsymbol{\tau}^s$, where

$$\boldsymbol{\tau}^v = \frac{1}{2} \int_V dV (\mathbf{r} \times \mathbf{M}) \quad (17)$$

is the volume term and the standard expression to evaluate the toroidal moment [3, 4], and

$$\boldsymbol{\tau}^s = -\frac{1}{10} \oint_S dS [\mathbf{r}(\mathbf{r} \cdot \mathbf{K}_b) - 2r^2 \mathbf{K}_b] \quad (18)$$

is the emergent toroidal moment due to surface-bound current \mathbf{K}_b . Notice that $\boldsymbol{\tau}^s$ is analogous to Eq. (1) but with a closed surface integral and opposite sign.

II. TOROIDAL MOMENTS OF THE STUDIED MAGNETIC TEXTURES

In this section, the volume and surface toroidal moments are calculated for various noncollinear magnetic states including the conical-helix textures in planar and tubular systems and skyrmionic magnetizations such as the skyrmion, bimeron and meron.

A. Analytical expressions for toroidal moments from conical-helix texture.

Using the model for the conical-helix texture magnetization described in the main text, the surface and volume toroidal moments, $\boldsymbol{\tau}^s$ and $\boldsymbol{\tau}^v$ respectively, calculated with respect to the geometric center of an ultrathin squared film with area L^2 and thickness d , are given by

$$\boldsymbol{\tau}^s = \sin \theta \begin{pmatrix} \mathcal{A}_1^s \sin \psi \cos \varphi_{\mathbf{q}} \\ -\mathcal{A}_1^s \sin \psi \sin \varphi_{\mathbf{q}} \\ \mathcal{A}_2^s \cos \psi \cos \varphi_{\mathbf{q}} \end{pmatrix} \quad (19)$$

and

$$\boldsymbol{\tau}^v = \mathcal{B}^v \sin \theta \begin{pmatrix} \sin \psi \cos \varphi_{\mathbf{q}} \\ -\sin \psi \sin \varphi_{\mathbf{q}} \\ \cos \psi \cos \varphi_{\mathbf{q}} \end{pmatrix}, \quad (20)$$

where $\mathcal{A}_1^s, \mathcal{A}_2^s$ and \mathcal{B}^v are

$$\mathcal{A}_1^s = \frac{M_s d L}{60 q^2} \left[(2d^2 q^2 + 7L^2 q^2 + 12) \sin \left(\frac{Lq}{2} \right) - 6Lq \cos \left(\frac{Lq}{2} \right) \right], \quad (21)$$

$$\mathcal{A}_2^s = \frac{M_s d L}{60 q^2} \left[(d^2 q^2 + 8L^2 q^2 + 12) \sin \left(\frac{Lq}{2} \right) - 6Lq \cos \left(\frac{Lq}{2} \right) \right], \quad (22)$$

$$\mathcal{B}^v = \frac{M_s d L}{2q^2} \left[Lq \cos \left(\frac{Lq}{2} \right) - 2 \sin \left(\frac{Lq}{2} \right) \right]. \quad (23)$$

An oscillatory behavior around $Lq/2$ is a prominent feature, which may result in positive, zero, or negative toroidal moments. In the ultrathin limit $L \gg d$, all the terms proportional to $(qd)^2$ are negligible. When comparing $\boldsymbol{\tau}^v$ with $\boldsymbol{\tau}^s$ it is interesting to note that despite their differences, the resulting toroidal moments are parallel to each other and always perpendicular to the respective pitch vector (\mathbf{q}) despite the choice of origin. Table I summarizes the toroidal moment directions for this texture and for both interfacial and bulk Dzyaloshinskii-Moriya interactions (b-DMI and i-DMI).

TABLE I. Summary of the surface toroidal moment directions for the conical helix with bulk and interfacial DMI and for the two relevant phase constants appropriate to in-plane ($\psi = \pi/2$) and out-of-plane ($\psi = 0$) magnetic films. The brackets show the pairs of surfaces contributing to $\boldsymbol{\tau}^s$.

Conical-helix	b-DMI	i-DMI
ψ	$(\varphi_{\mathbf{q}} = 0, \mathbf{q} = q \hat{y})$	$(\varphi_{\mathbf{q}} = \pi/2, \mathbf{q} = q \hat{x})$
$\pi/2$	$(\tau_x^s, 0, 0) \{S_x, S_y\}$	$(0, \tau_y^s, 0) \{S_x, S_y\}$
0	$(0, 0, \tau_z^s) \{S_y, S_z\}$	0

Fig. 1 shows the dependence of $\boldsymbol{\tau}^v$ with the lateral size L for fixed parameters and for both types of DMI. It can be seen that a difference between b-DMI ($\varphi_{\mathbf{q}} = 0$) and i-DMI ($\varphi_{\mathbf{q}} = \pi/2$) is the sign and the direction of $\boldsymbol{\tau}$ when $\psi = \pi/2$. For the other case, $\psi = 0$, a nonzero $\boldsymbol{\tau}$ is seen only for b-DMI, while for i-DMI, it cancels out. By analyzing the surface contribution, it is observed that for b-DMI, there is a slight difference in the amplitudes when comparing $\psi = 0$ and $\psi = \pi/2$, which is not the case for $\boldsymbol{\tau}^v$. In spite there is only one case in which $\boldsymbol{\tau}$ is always zero (for i-DMI and $\psi = 0$), for all other configurations of $\varphi_{\mathbf{q}}$ and ψ , the toroidal moment could be zero for specific values of $Lq/2$, which is due to commensurability. For the configurations studied, it is observed that $\boldsymbol{\tau}^v$ and $\boldsymbol{\tau}^s$ are always parallel to either x , y , or z depending on the type of DMI ($\varphi_{\mathbf{q}}$) and phase (ψ).

In order to describe the surface toroidal moment ($\boldsymbol{\tau}^s$) it is necessary to identify which faces contribute to its formation. Given the cuboid geometry of the sample, the surfaces are grouped by the direction of its normal vector, where S_x, S_y , and S_z refers to each pair of surfaces. Table I indicates the faces contributing to $\boldsymbol{\tau}^s$ in curly brackets. It is found, surprisingly, that for low perpendicular anisotropy ($\psi = \pi/2$), the surfaces contributing to $\boldsymbol{\tau}^s$ are the lateral edges (S_x, S_y) with area Ld . In contrast, for the surviving $\boldsymbol{\tau}$ when $\psi = 0$, the contributing pair of surfaces are S_y and S_z , where S_z have an area L^2 much larger than for $S_{x,y}$. From the point of view of the amplitudes, no significant difference is predicted when comparing $\psi = 0$ and $\psi = \pi/2$ for b-DMI as mentioned above; it is inferred then that the size of the areas is not particularly relevant, but rather the direction of their normal vectors.

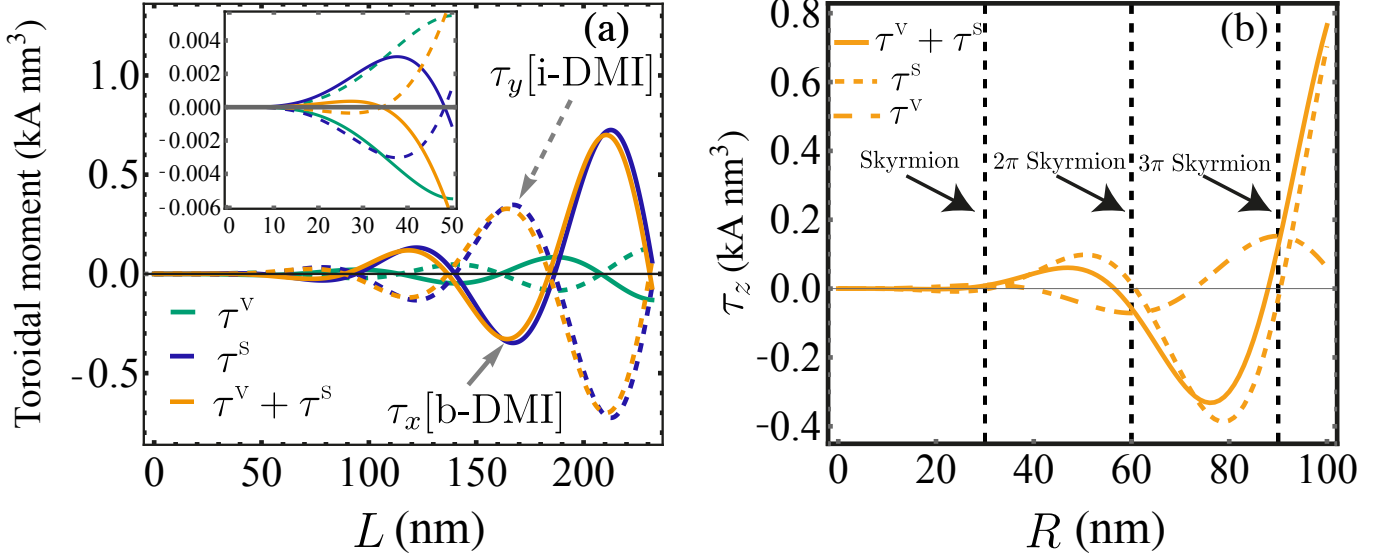


FIG. 1. (a) Nonzero components of the toroidal moments τ^v , τ^s , and their sum τ , for the conical-helix texture as a function of the film size L . The DMI strength is fixed at $D = 3 \text{ mJ/m}^2$, and the magnetic phase ($\psi = \pi/2$) correspond to a film with low perpendicular anisotropy. Continuous (segmented) curves correspond to bulk (interfacial) DMI with $x(y)$ -component, and the inset corresponds to a zoom of the first tens of nanometers. (b) Toroidal moments (z -component) for Bloch skyrmion-like states ($\gamma = \pi/2$) as a function of the nanodot radius when $\lambda = 30 \text{ nm}$.

B. Analytical expressions for toroidal moments from Skyrmion, bimeron and meron.

The chosen model for the skyrmionic textures is given by $\mathbf{M} = M_s [\sin \theta(\mathbf{r}) \cos(\phi + \gamma) \hat{x} + \sin \theta(\mathbf{r}) \sin(\phi + \gamma) \hat{y} + \cos \theta(\mathbf{r}) \hat{z}]$ [4], where $\theta(\mathbf{r}) = \pi(1 - r/\lambda)$, with λ a characteristic radius for which $\mathbf{M}(r = \lambda) = -\mathbf{M}(0)$, $0 \leq \phi \leq 2\pi$ and γ is the helicity: $\gamma = 0(\pi/2)$ corresponds to a Néel (Bloch) skyrmion. The same expression can describe the antiskyrmion, by making $\phi \rightarrow -\phi$, while the bimeron texture is obtained by considering a y -axis rotation in 90° , which implies $M_x \rightarrow M_z$, $M_y \rightarrow M_y$ and $M_z \rightarrow -M_x$. From this, it is possible to model Skyrmioniums or $\ell\pi$ -Skyrmions ($\ell = 1, 2, 3, \dots$) and $R = \ell\lambda$, which are skyrmion-like states stabilized in a ferromagnetic nanodisk of radius R and thickness d . They are composed of a combination of skyrmions or multiple full spin rotations along the diameter with a different topological charge [5–8]. We also considered a linear meron model [9], given by $\mathbf{M} = M_s [-\sin \theta(r) \sin \phi \hat{x} + \sin \theta(r) \cos \phi \hat{y} + \cos \theta(r) \hat{z}]$, where $\theta = \frac{\pi r}{2R}$ for $r \leq R$. Table II summarizes the volumetric and surface toroidal moments with their contributing faces and the Fig. 2 shows the dependence of the relevant components of τ^v with the helicity (γ). It can be seen from the Table II and the Fig. 2 that for $\gamma = 0$, τ^v is always zero, then Néel-like textures do not induce dipolar nonreciprocity. Note that full skyrmioniums are composed of integer values of ℓ ; however, a non-integer value was chosen in Fig. 2 for instructive reasons, since for integer values τ^s is always zero for bimerons.

TABLE II. Surface and volume toroidal moments for Skyrmion, bimeron, and meron. For antiskyrmion both toroidal moments are always zero. The brackets show the pairs of surfaces contributing to τ^s .

	Skyrmion	Bimeron	Meron
τ^s	$\mathcal{C}^s(0, 0, \sin \gamma) \{S_z\}$	$(\mathcal{D}_1^s \sin \gamma, \mathcal{D}_1^s \cos \gamma, \mathcal{D}_2^s \sin \gamma) \{S_z\}$	$(0, 0, \mathcal{E}^s) \{S_z, S_\rho\}$
τ^v	$\mathcal{C}^v(0, 0, \sin \gamma)$	$\mathcal{D}^v(\sin \gamma, \cos \gamma, \sin \gamma)$	$(0, 0, \mathcal{E}^v)$

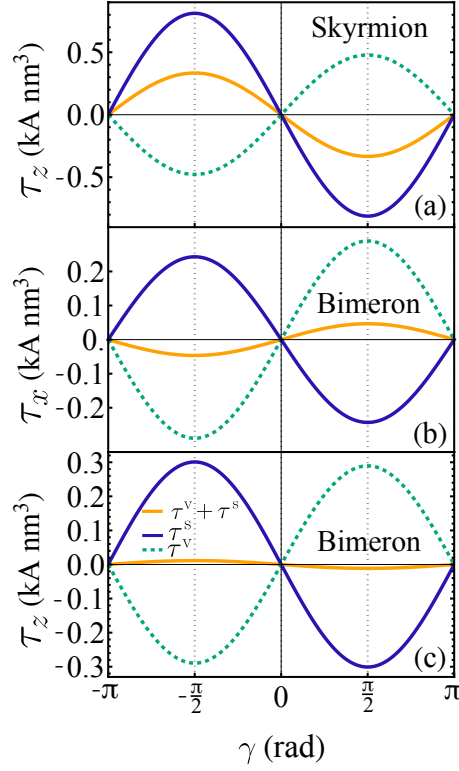


FIG. 2. Relevant components of the volume toroidal moment as a function of the magnetic helicity γ for different textures: (a) skyrmion (z -component) and (b,c) bimeron (x - and z -components) for $R = 100$ nm, $d = 1$ nm, $M_s = 658$ kA/m and $\lambda = 5R/4$.

The corresponding expressions that appears in Table II are

$$\mathcal{C}^s = -M_s d \frac{\pi R [\pi^2 d^2 + 24 (\lambda^2 + \pi^2 R^2)] \sin\left(\frac{\pi R}{\lambda}\right) - 24 \lambda^3 + 12 \lambda (2 \lambda^2 - \pi^2 R^2) \cos\left(\frac{\pi R}{\lambda}\right)}{60 \pi^2}, \quad (24)$$

$$\mathcal{C}^v = M_s d \lambda \frac{(2 \lambda^2 - \pi^2 R^2) \cos\left(\frac{\pi R}{\lambda}\right) - 2 \lambda [\lambda - \pi R \sin\left(\frac{\pi R}{\lambda}\right)]}{\pi^2}, \quad (25)$$

$$\mathcal{D}_1^s = -M_s \pi R d (d^2 + 12 R^2) \sin\left(\frac{\pi R}{\lambda}\right), \quad (26)$$

$$\mathcal{D}_2^s = -M_s d \frac{\pi R [\pi^2 d^2 + 24 (\lambda^2 + \pi^2 R^2)] \sin\left(\frac{\pi R}{\lambda}\right) - 24 \lambda^3 + 12 \lambda (2 \lambda^2 - \pi^2 R^2) \cos\left(\frac{\pi R}{\lambda}\right)}{120 \pi^2}, \quad (27)$$

$$\mathcal{D}^v = M_s d \lambda \frac{(2 \lambda^2 - \pi^2 R^2) \cos\left(\frac{\pi R}{\lambda}\right) - 2 \lambda [\lambda - \pi R \sin\left(\frac{\pi R}{\lambda}\right)]}{2 \pi^2}, \quad (28)$$

$$\mathcal{E}^s = -M_s d R \frac{\pi^3 d^2 + 24 R^2 (\pi^3 + 4 \pi - 8)}{60 \pi^2}, \quad (29)$$

$$\mathcal{E}^v = M_s d R^3 \frac{8(\pi - 2)}{\pi^2} \quad (30)$$

C. Toroidal moment of conical-helix texture on thin tubes

By considering the following model for a conical-helix magnetization distributed over a thin tubular shell [10],

$$\frac{\mathbf{M}}{M_s} = \cos(n\phi + q_z z + \psi) \sin \theta \hat{\rho} + \sin(n\phi + q_z z + \psi) \sin \theta \hat{\phi} + \cos \theta \hat{z} \quad (31)$$

where n is the azimuthal index which quantizes the azimuthal component of the pitch vector, q_z is the z -component of the pitch vector, ψ is a phase and θ is the cone angle.

the volume toroidal moment from Eq. 17 gives

$$\boldsymbol{\tau}^v = \frac{1}{2} \int dV \{ -z \sin \theta \sin(q_z z + n\phi + \psi) \hat{\rho} + [z \sin \theta \cos(q_z z + n\phi + \psi) - \rho \cos \theta] \hat{\phi} + \rho \sin \theta \sin(q_z z + n\phi + \psi) \hat{z} \}. \quad (32)$$

By changing from cylindrical to Cartesian unitary vectors, i.e., $(\hat{\rho}, \hat{\phi}, \hat{z}) \rightarrow (\hat{x}, \hat{y}, \hat{z})$, and integrating in cylindrical coordinates for a thin tube with inner radius βR , outer radius R and length L , $\boldsymbol{\tau}^v$ becomes

$$\begin{aligned} \boldsymbol{\tau}^v = M_s R^2 \sin \theta \sin(n\pi) \left\{ \frac{(1 - \beta^2) \cos(n\pi + \psi)}{2q_z^2(n+1)} \left[q_z L \cos\left(\frac{q_z L}{2}\right) - 2 \sin\left(\frac{q_z L}{2}\right) \right] \hat{x} \right. \\ \left. + \frac{(1 - \beta^2) \sin(n\pi + \psi)}{2q_z^2(n+1)} \left[q_z L \cos\left(\frac{q_z L}{2}\right) - 2 \sin\left(\frac{q_z L}{2}\right) \right] \hat{y} \right. \\ \left. + \frac{2(1 - \beta^3) R}{3q_z n} \sin\left(\frac{q_z L}{2}\right) \sin(n\pi + \psi) \hat{z} \right\}. \end{aligned} \quad (33)$$

By inspecting the q_z and n values it is found that this expression is only nonzero for $n = 0$ and $n = -1$ and the result can be expressed as

$$\begin{aligned} \boldsymbol{\tau}^v = M_s \frac{2\pi(1 - \beta^3) R^3}{3q_z} \sin \theta \sin \psi \sin\left(\frac{q_z L}{2}\right) \delta_{n,0} \hat{z} \\ + M_s \frac{\pi R^2(1 - \beta^2)}{2q_z^2} \sin \theta \left[q_z L \cos\left(\frac{q_z L}{2}\right) - 2 \sin\left(\frac{q_z L}{2}\right) \right] \delta_{n,-1} (\cos \psi \hat{x} + \sin \psi \hat{y}). \end{aligned} \quad (34)$$

where the symbol $\delta_{i,j}$ denotes the Kronecker delta function. For the particular case $q_z = 0$ and $n = 0$,

$$\boldsymbol{\tau}^v = M_s \frac{LR^3}{3} \pi (1 - \beta^3) \sin \theta \sin \psi \hat{z}. \quad (35)$$

On the other hand, the toroidal moment $\boldsymbol{\tau}$ (Eq. 1) for the same texture is given by,

$$\begin{aligned} \boldsymbol{\tau} = \frac{M_s \pi (\beta - 1) R \sin \theta \sin \psi}{30q_z^3} \left[\sin\left(\frac{q_z L}{2}\right) (q_z^2 (3L^2 + 4(\beta^2 + \beta + 1) R^2) - 24) \right. \\ \left. + 2q_z L \cos\left(\frac{q_z L}{2}\right) ((\beta^2 + \beta + 1) q_z^2 R^2 + 6) \right] \hat{z} \delta_{n,0} \\ - \frac{M_s \pi (\beta^2 - 1) R^2 \sin \theta}{20q_z^2} \left[\sin\left(\frac{q_z L}{2}\right) (q_z^2 (2L^2 + 3(\beta^2 + 1) R^2) - 16) + 8q_z L \cos\left(\frac{q_z L}{2}\right) \right] (\cos \psi \hat{x} + \sin \psi \hat{y}) \delta_{n,-1} \\ + \frac{M_s \pi (\beta^2 - 1) R^2 \sin \theta}{20q_z^2} \left[\sin\left(\frac{q_z L}{2}\right) ((\beta^2 + 1) q_z^2 R^2 - 4) + 2q_z L \cos\left(\frac{q_z L}{2}\right) \right] (\cos \psi \hat{x} - \sin \psi \hat{y}) \delta_{n,1}. \end{aligned} \quad (36)$$

This last expression is only nonzero for $n = -1$, $n = 0$ and $n = 1$. Analogously, the surface toroidal moment $\boldsymbol{\tau}^s$ for this texture using the Eq. 18 is

$$\begin{aligned} \boldsymbol{\tau}^s = \frac{M_s \pi (\beta - 1) R \sin \theta \sin \psi}{30q_z^3} \left[3 \sin\left(\frac{q_z L}{2}\right) (q_z^2 (L^2 + 8(\beta^2 + \beta + 1) R^2) - 8) \right. \\ \left. + 2q_z L \cos\left(\frac{q_z L}{2}\right) ((\beta^2 + \beta + 1) q_z^2 R^2 + 6) \right] \hat{z} \delta_{n,0} \\ - \frac{M_s \pi (\beta^2 - 1) R^2 \sin \theta \cos \psi}{20q_z^2} \left[\sin\left(\frac{q_z L}{2}\right) (q_z^2 (2L^2 + 3(\beta^2 + 1) R^2) + 4) - 2q_z L \cos\left(\frac{q_z L}{2}\right) \right] \\ \times (\cos \psi \hat{x} + \sin \psi \hat{y}) \delta_{n,-1} \\ + \frac{M_s \pi (\beta^2 - 1) R^2 \sin \theta}{20q_z^2} \left[\sin\left(\frac{q_z L}{2}\right) ((\beta^2 + 1) q_z^2 R^2 - 4) + 2q_z L \cos\left(\frac{q_z L}{2}\right) \right] (\cos \psi \hat{x} - \sin \psi \hat{y}) \delta_{n,1}. \end{aligned} \quad (37)$$

which, as (36), is only non-zero for $n = 0$, $n = -1$ and $n = 1$. It can be noticed that the terms associated with $n = 1$ are exactly the same for $\boldsymbol{\tau}$ and $\boldsymbol{\tau}^s$ and because of that, those terms do not appear for $\boldsymbol{\tau}^v$.

- [2] D. J. Griffiths, *Introduction to electrodynamics* (Pearson, 2013).
- [3] N. A. Spaldin, M. Fiebig, and M. Mostovoy, The toroidal moment in condensed-matter physics and its relation to the magnetoelectric effect, [J. Phys. Condens. Matter. **20**, 434203 \(2008\)](#).
- [4] S. Bhowal and N. A. Spaldin, Magnetoelectric classification of skyrmions, [Phys. Rev. Lett. **128**, 227204 \(2022\)](#).
- [5] R. A. Pepper, M. Beg, D. Cortés-Ortuño, T. Kluyver, M.-A. Bisotti, R. Carey, M. Vousden, M. Albert, W. Wang, O. Hovorka, and H. Fangohr, Skyrmion states in thin confined polygonal nanostructures, [Journal of Applied Physics **123**, 093903 \(2018\)](#).
- [6] D. Cortés-Ortuño, N. Romming, M. Beg, K. von Bergmann, A. Kubetzka, O. Hovorka, H. Fangohr, and R. Wiesendanger, Nanoscale magnetic skyrmions and target states in confined geometries, [Phys. Rev. B **99**, 214408 \(2019\)](#).
- [7] N. Mehmood, R. Fazal, W. Yadong, T. Guo, Q. Zhang, Z. Hou, G. Xingsen, and J.-M. Liu, Stability phase diagrams and tuning of magnetic skyrmionium and other states, [Journal of Magnetism and Magnetic Materials **526**, 167706 \(2021\)](#).
- [8] M. Ponsudana, R. Amuda, R. Madhumathi, A. Brinda, and N. Kanimozhi, Confinement of stable skyrmionium and skyrmion state in ultrathin nanoring, [Physica B: Condensed Matter **618**, 413144 \(2021\)](#).
- [9] P. G. Radaelli, J. Radaelli, N. Waterfield-Price, and R. D. Johnson, Micromagnetic modeling and imaging of vortex|meron structures in an oxide|metal heterostructure, [Phys. Rev. B **101**, 144420 \(2020\)](#).
- [10] B. Mimiça-Figari, F. Brevis, D. Cortés-Ortuño, R. A. Gallardo, and P. Landeros, Magnetic textures in nanotubes with interfacial Dzyaloshinskii-Moriya interaction, unpublished (2024).